Inorg. Chem. **2002**, *41*, 4627−4629

Molecular Structures of Five-Coordinated Halide Ligated Iron(III) Porphyrin, Porphycene, and Corrphycene Complexes

Yoshiki Ohgo,[†] Saburo Neya,[⊥] Takahisa Ikeue,[†] Masashi Takahashi,[‡] Masuo Takeda,[‡] Noriaki Funasaki,[§] and Mikio Nakamura*[,†,∥]

Department of Chemistry, School of Medicine, Toho University, Ota-ku, Tokyo 143-8540, Japan, Department of Physical Chemistry, Faculty of Pharmaceutical Sciences, Chiba University, Chiba 263-8522, Japan, Department of Chemistry, Faculty of Science, Toho University, Funabashi 274-8510, Japan, Department of Physical Chemistry, Kyoto Pharmaceutical University, Kyoto 607-8414, Japan, and Division of Biomolecular Science, Graduate School of Science, Toho University, Funabashi, Chiba 274-8510, Japan.

Received April 30, 2002

Molecular structures of 12 porphyrin analogues, Fe^{III}(EtioP)X(**1**$_a$–**1**$_d$), Fe^{III}(EtioCn)X(**2**$_a$–**2**$_d$), and Fe^{III}(Etio-Pc)X(**3**$_a$–**3**$_d$), where X = F (**a**), Cl (**b**), Br (**c**), and I (**d**), are determined on the basis of X-ray crystallography. Combined analyses using Mössbauer, ^{1}H NMR, and EPR spectroscopy as well as SQUID magnetometry have revealed that **3**$_d$ exhibits a quite pure $S = {}^3/_2$ spin state with a small amount of an $S = {}^5/_2$ spin admixture. In contrast, all the other complexes show the $S = {}^5/_2$ spin state with a small amount of the $S = {}^3/_2$ spin admixture. The structural and spectroscopic data indicate a strong correlation between the spin states of the complexes and the core geometries such as Fe–N bond lengths, cavity areas, and ΔFe values.

Studies on the porphyrin analogues such as corroles, porphycenes, N-confused porphyrins, expanded porphyrins, and so forth have attracted much attention because they show quite unique physicochemical properties different from those of porphyrins.[1−3] Elucidation of the basic properties of porphyrin analogues is quite important not only for the deeper understanding of the biologically important iron(III) porphyrins but for the potential application of these compounds to new areas such as photodynamic therapy.[4] Here, we report on the structural characteristics of five-coordinated iron(III) halides of etioporphyrins (**1**), etiocorrphycenes (**2**), and etioporphycenes (**3**) on the basis of crystallographic analyses of the 12 complexes.

Fe^{III}(EtioP)X(**1**$_a$−**1**$_d$), Fe^{III}(EtioCn)X(**2**$_a$−**2**$_d$), and Fe^{III}(EtioPc)X (**3**$_a$−**3**$_d$),[5] where X = F (**a**), Cl (**b**), Br (**c**), and I (**d**), were synthesized according to the reported method.[6−9] Table 1 summarizes the structural parameters of the 12 complexes. Figure 1 shows the molecular structures of the

Table 1. Some Structural Data

complex	Fe−N$_p$ [Å]	Fe−X [Å]	cavity area [Å^2]	ΔFe [Å]	Δ_{max} [Å]
1a	2.058(2)	1.836(2)	8.123	0.409(1)	0.09
1b	2.061(4)	2.241(1)	8.094	0.444(2)	0.05
1c[a]	2.052(6)	2.338(1)	8.023	0.440(3)	0.06
1d	2.061(7)	2.617(1)	8.094	0.454(4)	0.22
2a	2.026(3)	1.938(2)	7.784	0.423(1)	0.12
	2.049(3)				
2b	2.048(2)	2.247(1)	7.813	0.431(2)	0.14
	2.068(2)				
2c	2.014(4)	2.399(1)	7.866	0.420(2)	0.20
	2.062(4)				
2d	2.034(2)	2.615(1)	7.897	0.387(1)	0.35
	2.056(2)				
3a	2.020(3)	2.259(1)	7.539	0.524(1)	0.39
3b[b]	2.027(3)	2.232(1)	7.497	0.532(2)	0.39
3c	1.998(3)	2.412(1)	7.475	0.450(1)	0.39
3d	1.956(3)	2.664(1)	7.355	0.343(2)	0.36

[a] The average values of two independent molecules. [b] Previously reported data.[14]

* To whom correspondence should be addressed. E-mail: mnakamu@med.toho-u.ac.jp.
[†] School of Medicine, Toho University.
[⊥] Chiba University.
[‡] Faculty of Science, Toho University.
[§] Kyoto Pharmaceutical University.
[∥] Graduate School of Science, Toho University.

(1) Sessler, J. L.; Gebauer, A.; Vogel, E. In *The Porphyrin Handbook*; Kadish, K. M., Smith, K. M., Guilard R., Eds.; Academic Press: San Diego, CA, 2000; Vol. 2, pp 1−54.
(2) Erben, C.; Will, S.; Kadish, K. M. In *The Porphyrin Handbook*; Kadish, K. M., Smith, K. M., Guilard R., Eds.; Academic Press: San Diego, CA, 2000; Vol. 2, pp 233−300.
(3) Gross, Z.; Golubkov, G.; Simkhovich, L. *Angew. Chem., Int. Ed.* **2000**, *39*, 4045−4047.
(4) Szeismies, R. M.; Calzabara-Pinton, P. G.; Karrer, S.; Ortel, B.; Landthaler, M. *J. Photochem. Photobiol., B* **1996**, *36*, 213−219.
(5) Abbreviations: EtioP, EtioCn, EtioPc, and TPrPc are dianions of 2,7,-12,17-tetraethyl-3,8,13,18-tetramethylporphyrin, 2,7,12,17-tetraethyl-3,6,11,18-tetramethylcorrphycene, 3,6,13,16-tetraethyl-2,7,12,17-tetramethylporphycene, and 2,7,12,17-tetrapropylporphycene.
(6) Fuhrhop, J.-H.; Smith K. M. In *Porphyrins and Metalloporphyrins*, Elsevier: Amsterdam, 1975; pp 757−869.
(7) Neya, S.; Nishinaga, K.; Ohyama, K.; Funasaki, N. *Tetrahedron Lett.* **1998**, *39*, 5217−5220.
(8) Vogel, E.; Koch, P.; Hou, X.-L.; Lex, J.; Lausmann, M.; Kisters, M.; Aukauloo, M. A.; Richard, P.; Guilard, R. *Angew. Chem., Int. Ed. Engl.* **1993**, *32*, 1600−1604; *Angew. Chem.* **1993**, *105*, 1670−1673.
(9) Maricondi, C.; Swift, W.; Straub, D. K. *J. Am. Chem. Soc.* **1969**, *91*, 5205−5210.

10.1021/ic0256866 CCC: $22.00
Published on Web 08/14/2002

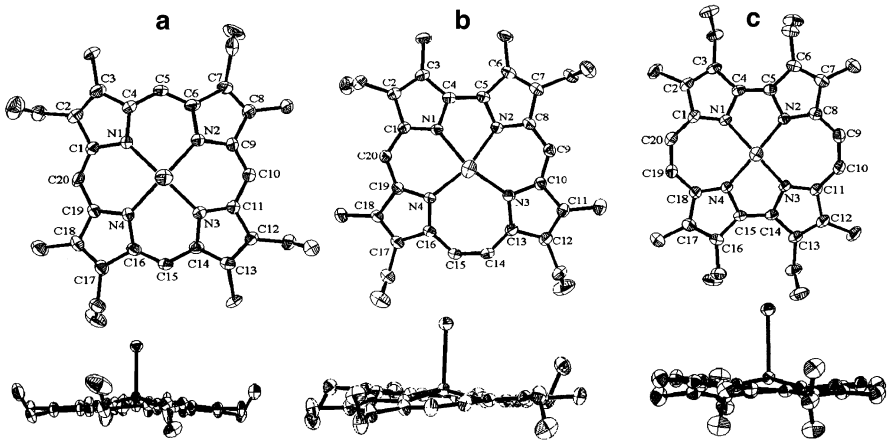

Figure 1. ORTEP diagrams with atomic numbering of (a) **1d**, (b) **2d**, and (c) **3d** viewed along the Fe−I bond. Corresponding side views are shown in the lower row. Displacement ellipsoids are shown at 30% probability level. H-atoms are omitted for clarity.

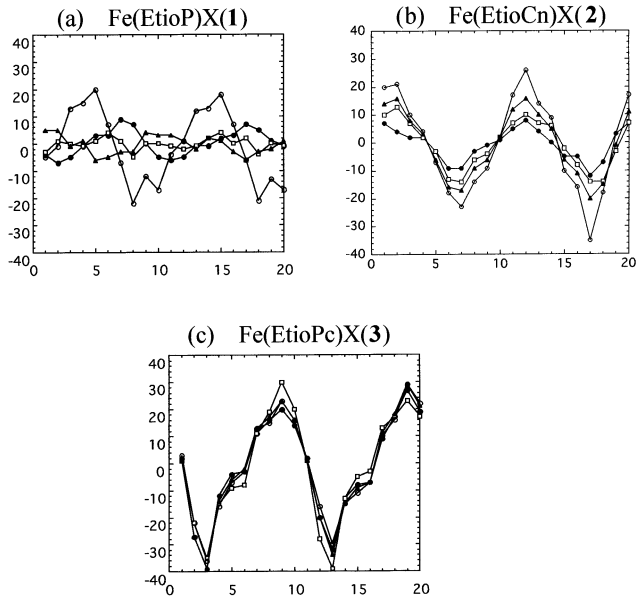

Figure 2. Displacements of the peripheral carbon atoms from the mean plane of the 24 atoms in (a) **1**, (b) **2**, and (c) **3**: X = F^- (●); X = Cl^- (□); X = Br^- (▲); X = I^- (○).

iodide complexes, $\mathbf{1_d}$, $\mathbf{2_d}$, and $\mathbf{3_d}$, as typical examples. Similar to the corresponding free-bases, the N4 cores show square, trapezoidal, and rectangular shapes for **1**, **2**, and **3**, respectively. The data in Table 1 reveal several structural characteristics for these complexes. The average Fe−N_p lengths are the longest in **1** followed by **2** and **3** for the same axial ligand. The difference in the average Fe−N_p lengths should be reflected in the cavity sizes of these complexes. Thus, we calculated the cavity areas surrounded by the four nitrogen atoms. As expected, the cavity areas of **1** are in the range 8.023−8.123 Å^2 and are larger than those of **2**, 7.784−7.897 Å^2, and **3**, 7.255−7.539 Å^2. Close examination of the data in Table 1 reveals that, while the cavity area of **2** gradually increases on going from F^- to Cl^-, to Br^-, and then to I^-, that of **3** has shown a considerable decrease for the same change of the axial ligands. In contrast, no clear tendency has been observed in the case of **1**. Similar discrepancies among the three types of complexes are observed in the ΔFe value defined by the perpendicular displacement of the iron(III) atom from the least-squares plane of the central four nitrogen atoms. Although the ΔFe value increases gradually in **1** as the axial ligand changes from F^- to I^-, it decreases both in **2** and **3** for the same change of the axial ligand. It should be noted that the decrease in **3** is fairly large, 0.181 Å, which corresponds to the 35% decrease.

Figure 2 shows the vertical displacements of the peripheral carbon atoms from the mean plane of the 24 atoms. While the porphyrin rings of **1** are rather planar except for that of $\mathbf{1_d}$, those of **2** and **3** are much more distorted. The magnitude of distortion can also be estimated by the Δ_{max} values defined by the largest displacement of the peripheral carbon atoms from the mean porphyrinoid plane, and they are listed in Table 1. Figure 2 clearly indicates that the degree of deformation in **3** is almost the same regardless of the axial halides. In contrast, the degree of deformation in **1** and **2** is appreciably different depending on the axial halides. Particularly noticeable are the ring conformations of **1** in the sense that only $\mathbf{1_d}$ shows a deformed structure with the Δ_{max} value of 0.22 Å; $\mathbf{1_a}$−$\mathbf{1_c}$ exhibit nearly planar structures with Δ_{max} values less than 0.09 Å. It is surprising that $\mathbf{3_a}$−$\mathbf{3_d}$ maintain the similarly deformed ring conformation despite the large difference in the cavity areas and ΔFe values. The result could be explained in terms of the severe steric repulsion between the ethyl groups at C3 and C6 positions; the steric repulsion deforms the porphycene ring to such an extent that the change in axial ligand can no longer affect the ring conformation.

The structural characteristics mentioned here should affect the physicochemical properties such as spectroscopic, magnetic, and redox behaviors. As one of the examples, we have examined the spin states of these complexes. The effective magnetic moments (μ_{eff}) determined by the SQUID magnetometry for the microcrystalline samples of chlorides and iodides are given in Table 2. While $\mathbf{3_d}$ exhibits the $S = {}^3/_2$ spin state with a small amount of $S = {}^5/_2$ spin admixture, other complexes show the $S = {}^5/_2$ spin state with a small amount of $S = {}^3/_2$ spin admixture. The data in Table 2 also indicate that the iodides have much larger $S = {}^3/_2$ mixing than the corresponding chlorides; the μ_{eff} values of $\mathbf{1_d}$ and

Table 2. Spectroscopic and Magnetic Data

		Mössbauer[b]		EPR[c]		^{1}H NMR[d]		
complex	SQUID[a] μ_{eff} (μ_B)	IS (mm s^{-1})	QS (mm s^{-1})	$g_\perp$	$g_\parallel$	meso	etheno	CH_3
1b	5.80 (5.79)	0.20 (0.26)	0.63 (0.55)	5.89	2.00	−55.6		52.2
2b	5.79 (5.61)	0.30 (0.40)	1.17 (1.29)	5.90[e]	2.00	−33.8	27.5	76.0 66.0
3b	5.66 (5.42)	0.25 (0.39)	1.24 (1.36)	5.10	2.00		−11.7	42.5
1d	5.42 (5.35)	0.23 (0.42)	0.90 (1.14)	5.82	1.98	−47.5		60.2
2d	5.19 (5.03)	0.32 (0.43)	1.50 (1.52)	5.88[f]	1.95	−26.2	37.0	83.0 69.4
3d	4.21 (3.65)	0.21 (0.29)	3.02 (3.25)	4.10[g]	1.96		0.4	43.0

[a] Data at 300 K. Data at 70 K are in the parentheses. [b] Data at 279 K. Data at 77 K are in the parentheses. [c] Data at 4.2 K in frozen CH_2Cl_2 solution. [d] Chemical shifts (δ, ppm) at 298 K in CD_2Cl_2 solution. [e] $g_x = 6.30$, $g_y = 5.50$. [f] $g_x = 6.25$, $g_y = 5.50$. [g] $g_x = 4.30$, $g_y = 3.90$.

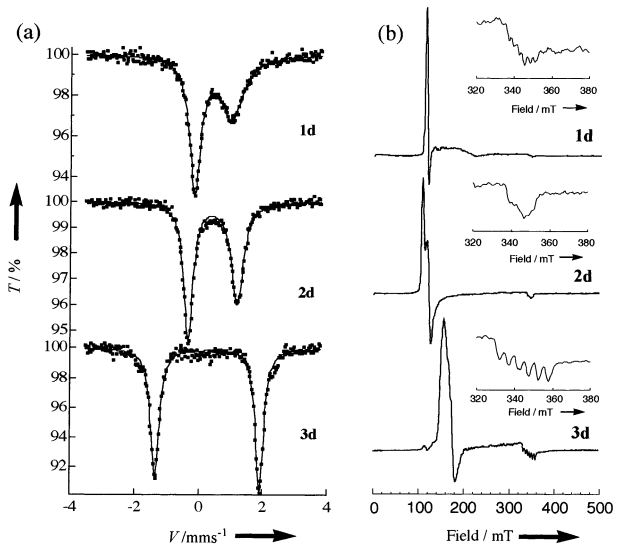

Figure 3. (a) Mössbauer (microcrystalline, 297 K) and (b) EPR (CH_2Cl_2, 4.2 K) spectra of **1d**, **2d**, and **3d**.

2d at 300 K are 5.42 and 5.19 μ_B, respectively, as compared with 5.80 and 5.79 μ_B in **1b** and **2b**. To further confirm the spin states, the Mössbauer spectra were measured for the microcrystalline samples over the temperature range 77−297 K. Table 2 lists the isomer shift (IS) values and quadrupole splitting (QS) values determined at 77 and 297 K. The Mössbauer spectra of the iodides taken at 297 K are shown in Figure 3a as typical examples. The QS values, which reflect the iron(III) spin state, increase on going from **1** to **3** for the chlorides and iodides. The QS value of an iodide complex is much larger than that of the corresponding chloride complex for each macrocycle. In the case of **3d**, the QS value reaches as much as 3.02 mm s^{-1} at ambient temperature, suggesting strongly that the complex adopts the $S = {}^3/_2$ with a small mixing of the $S = {}^5/_2$.[10,11] Thus, both the Mössbauer and SQUID results indicate that the $S = {}^3/_2$ character increases in the order **1** < **2** ≪ **3** for each halide and also increases in the order Cl^- < I^- for each macrocycle. The large $S = {}^3/_2$ character in **3**, especially that in **3d**, can be explained in terms of the destabilization of the $d_{x^2-y^2}$ and $d_\pi(d_{xz}, d_{yz})$ orbitals because of the small cavity area determined by the Fe−N_p bond length and the cavity shape of the N4 core together with the small ΔFe value. Weak axial ligation as is revealed from the longer Fe−X bond in **3** should lower the d_{z^2} orbital and contribute to the further stabilization of the $S = {}^3/_2$ spin state.[11]

To reveal the spin states of these complexes in solution, we have measured the EPR spectra in frozen $CHCl_3$ solution at 4.2 K and determined the g values as listed in Table 2. Figure 3b shows the EPR spectra of the iodide complexes. Hyperfine coupling with axially coordinated iodide, 48.9 G, is clearly observed in the case of **3d**. Consistent with the SQUID and Mössbauer results, **3d** shows a quite pure $S = {}^3/_2$ spin state as is revealed from $g_\perp = 4.10$; the $S = {}^3/_2$ contribution in the quantum-mechanical $S = {}^5/_2$, ${}^3/_2$ spin admixing system is calculated to be 94%.[12] Even the chloride complex **3b** shows a 38% $S = {}^3/_2$ spin admixture. In contrast, the $S = {}^3/_2$ contribution in **1** and **2** is rather small. We have then examined the ^{1}H NMR spectra in CD_2Cl_2 solution. The chemical shifts at 300 K are listed in Table 2. In the case of porphycene complexes, the etheno protons are the useful probe to determine the spin state. The chemical shifts are −16.0 (not shown), −11.7, −5.22 (not shown), and 0.36 ppm for **3a**−**3d**, respectively. Because the chemical shift of **3d** is close to that of the pure intermediate spin complexes, [Fe^{III}(TPrPc)(THF)$_2$]ClO_4 and [Fe^{III}(TPrPc)]ClO_4,[10,13] the downfield shift of the etheno signal on going from **3a** to **3d** corresponds to the increase in the $S = {}^3/_2$ character.[13] The etheno protons of the corrphycene complexes could also be good probes though the chemical shifts are somehow scattered: −27.2 (not shown), −33.8, −32.4 (not shown), and −26.2 ppm for **2a**−**2d**, respectively. Molecular orbital calculations in conjunction with the structural data determined by the present study could reveal the spin distribution on the corrphycene ring, which enables the relationship between the spin state and NMR chemical shifts in **2**. These studies are now in progress in this group.

Acknowledgment. We thank Professors Yuji Ohashi and Hidehiro Uekusa, Department of Chemistry, Faculty of Science, Tokyo Institute of Technology, for assistance during the X-ray measurements. This work was supported by the Grant in Aid for Scientific Research on Priority Areas(A) (No. 12020257 to M.N.) from Ministry of Education, Culture, Sports, Science and Technology, Japan. The authors are grateful to Mr. Masahiro Sakai of the IMS for assistance with EPR and SQUID measurements.

Supporting Information Available: Crystallographic information file (CIF). This material is available free of charge via the Internet at http://pubs.acs.org.

IC0256866

(10) Ikeue, T.; Ohgo, Y.; Takahashi, M.; Takeda, M.; Neya, S.; Funasaki, N.; Nakamura, M. *Inorg. Chem.* **2001**, *40*, 3650−3652.
(11) Ikeue, T.; Ohgo, Y.; Yamaguchi, T.; Takahashi, M.; Takeda, M.; Nakamura, M. *Angew. Chem., Int. Ed.* **2001**, *40*, 2617−2620; *Angew. Chem.* **2001**, *113*, 2687−2690.
(12) Palmer, G. In *Iron Porphyrins, Part II*; Lever, A. B., Gray H. B., Eds.; Addison-Wesley: Reading, MA, 1983; pp 43−88.
(13) Rachlewicz, K.; Latos-Grażyński, L.; Vogel, E.; Ciunik, Z.; Jerzykiewicz, L. B. *Inorg. Chem.* **2002**, *41*, 1979−1988.
(14) Ohgo, Y.; Neya, S.; Ikeue, T.; Funasaki, N.; Nakamura, M. *Acta Crystallogr.* **2001**, *C57*, 1046−1047.